

**A DETERMINATION OF THE STRONG COUPLING CONSTANT
 α_s FROM W PRODUCTION AT THE CERN $p\bar{p}$ COLLIDER**

The UA2 Collaboration

Bern - Cambridge - CERN - Dortmund - Heidelberg - Melbourne -
Milano - Orsay (LAL) - Pavia - Perugia - Pisa - Saclay (CEN)

J.Alitti¹², G.Ambrosini⁹, R.Ansari⁸, D.Autiero¹¹, P.Bareyre¹², I.A.Bertram⁶,
G.Blalock^{3,a}, P.Bonamy¹², M.Bonesini⁷, K.Borer¹, M.Bourlialud¹², D.Buskulic⁸,
G.Carboni¹¹, D.Cavalli⁷, V.Cavasinni¹¹, P.Cenci¹⁰, J.C.Chollet⁸, C.Conta⁹, G.Costa⁷,
F.Costantini¹¹, L.Cozzi⁷, A.Craverio⁷, M.Curatolo¹¹, A.Dell'Acqua⁹, T.DelPrete¹¹,
R.S.DeWolf², L.DiLella³, Y.Ducros¹², G.F.Egan⁶, K.F.Einsweiler^{3,b}, B.Esposito¹¹,
L.Fayard⁸, A.Federspiel¹, R.Ferrari⁹, M.Fraternali^{9,c}, D.Froidevaux³, G.Fumagalli⁹,
J.M.Gaillard⁸, F.Gianotti⁷, O.Gildemeister³, C.Gössling⁴, V.G.Goggi⁹,
S.Grünendahl⁵, K.Hara^{1,d}, S.Hellman³, J.Hrivnac³, H.Hufnagel⁴, E.Hugentobler¹,
K.Hultqvist^{3,e}, E.Iacopini^{11,f}, J.Incandela⁷, K.Jakobs³, P.Jenni³, E.E.Kluge⁵,
N.Kurz⁵, S.Lami¹¹, P.Lariccia¹⁰, M.Lefebvre³, L.Linssen³, M.Livan^{9,g},
P.Lubrano^{3,10}, C.Magneville¹², L.Mandelli⁷, L.Mapelli³, M.Mazzanti⁷, K.Meier^{3,h},
B.Merkel⁸, J.P.Meyer¹², M.Moniez⁸, R.Moning¹, M.Morganti^{11,i}, L.Müller¹,
D.J.Munday², M.Nessi³, F.Nessi-Tedaldi³, C.Onions³, T.Pal¹, M.A.Parker²,
G.Parrour⁸, F.Pastore⁹, E.Pennacchio⁹, J.M.Pentney³, M.Pepe³, L.Perini^{7,c},
C.Petridou¹¹, P.Petroff⁸, H.Plochow-Besch³, G.Polesello^{3,9}, A.Poppleton³, K.Pretzl¹,
M.Primavera^{11,j}, M.Punturo¹⁰, J.P.Repellin⁸, A.Rimoldi⁹, M.Sacchi⁹, P.Scampoli¹⁰,
J.Schacher¹, V.Simak³, S.L.Singh², V.Sondermann⁴, S.Stapnes³, A.V.Stirling¹²,
C.Talamonti¹⁰, F.Tondini¹⁰, S.N.Tovey⁶, E.Tsesmelis⁴, G.Unal⁸,
M.Valdata-Nappi^{11,j}, V.Vercesi⁹, A.R.Weidberg^{3,k}, P.S.Wells^{2,l}, T.O.White²,
D.R.Wood⁸, S.A.Wotton^{2,l}, H.Zaccone¹², A.Zylberstein¹²

(Submitted to Physics Letters)

Abstract

The large sample of $W \rightarrow e\nu$ events collected by the UA2 experiment at the CERN $p\bar{p}$ collider between 1988 and 1990 has been used to determine the strong coupling constant α_s . From a measurement of the ratio of the production rate of W events with one jet to that with no jets, α_s has been extracted to second order in the \overline{MS} scheme : $\alpha_s(M_W^2) = 0.123 \pm 0.018$ (stat.) ± 0.017 (syst.).

- 1 Laboratorium für Hochenergiephysik, Universität Bern, Sidlerstraße 5, 3012 Bern, Switzerland
 - 2 Cavendish Laboratory, University of Cambridge, Cambridge, CB3 0HE, UK
 - 3 CERN, 1211 Geneva 23, Switzerland
 - 4 Lehrstuhl für Exp. Physik IV, Universität Dortmund, 4600 Dortmund, FRG
 - 5 Institut für Hochenergiephysik der Universität Heidelberg, Schröderstraße 90, 6900 Heidelberg, FRG
 - 6 School of Physics, University of Melbourne, Parkville 3052, Australia.
 - 7 Dipartimento di Fisica dell'Università di Milano and Sezione INFN Milano, 20133 Milano, Italy
 - 8 Laboratoire de l'Accélérateur Linéaire, Université de Paris-Sud, 91405 Orsay, France
 - 9 Dipartimento di Fisica Nucleare e Teorica, Università di Pavia and INFN, Sezione di Pavia, Via Bassi 6, 27100 Pavia, Italy
 - 10 Dipartimento di Fisica dell'Università di Perugia and INFN, Sezione di Perugia, via Pascoli, 06100 Perugia, Italy
 - 11 Dipartimento di Fisica dell'Università di Pisa and INFN, Sezione di Pisa, Via Livornese, S.Piero a Grado, 56100 Pisa, Italy
 - 12 Centre d'Etudes Nucléaires de Saclay, 91191 Gif-sur-Yvette Cedex, France
- a) Now at University of California, Santa Cruz, California, USA
 - b) Now at Lawrence Berkeley Laboratory, Berkeley, California, USA
 - c) Now at Istituto di Fisica, Università di Palermo, Italy
 - d) Now at University of Tsukuba, Tsukuba, Ibaraki 305, Japan
 - e) Now at University of Stockholm, Stockholm, Sweden
 - f) Also at Scuola Normale Superiore, Pisa, Italy
 - g) Now at Dipartimento di Fisica, Università di Cagliari, Italy
 - h) Now at Deutsches Elektronen Synchrotron, Hamburg, FRG
 - i) Now at Dipartimento di Fisica e INFN di Bologna, Università Bologna, Italy
 - j) Now at Dipartimento di Fisica dell'Università della Calabria e gruppo INFN, Cosenza, Italy
 - k) Now at Nuclear Physics Laboratory, University of Oxford, Oxford, UK
 - l) Now at CERN, Geneva, Switzerland.

1. INTRODUCTION

The production of W bosons in $p\bar{p}$ collisions is described to leading order in perturbation theory by the Drell-Yan mechanism. The strong interaction accounts for corrections leading to the associated production of W bosons and hadron jets. The dependence of the rate of W + jet events on the strong coupling constant α_s can be used to measure its value in hadronic collisions. In analogy to an analysis performed by the UA2 collaboration with data taken in the years 1981 to 1985 [1], a variable R is considered, which is defined as the ratio of the number of W + one-jet to W + zero-jet events. A value of α_s is extracted from a comparison of the experimental value R_{EXP} to the value R_{MC} predicted by a Monte Carlo calculation based on Quantum Chromodynamics (QCD).

The new W data sample, collected by the upgraded UA2 experiment in the data taking periods between 1988 and 1990 at the CERN $p\bar{p}$ collider ($\sqrt{s} = 630$ GeV), which corresponds to an integrated luminosity of 13 pb^{-1} , allows for a more significant comparison between data and QCD predictions, with reduced statistical and systematic uncertainties, compared to the previous analysis [1]. The jet identification, which was reliable only in the pseudorapidity range $|\eta| < 0.85$ in the previous analysis, can be extended to larger rapidities covered by the new end cap calorimeters of the upgraded detector [2]. In order to define jets experimentally, a higher transverse energy threshold can be used, resulting in reduced experimental systematic uncertainties. This also guarantees that the comparison between data and theory is done in a kinematical region where perturbative QCD calculations are expected to be reliable. On the theoretical side, the recent complete calculation of the total W production cross section to second order in α_s [3,4], and the complete second order calculation of the P_T^W spectrum [5] can be used to obtain an exact calculation of the topological K-factors needed to correct the tree level Monte Carlo predictions for higher order contributions. In this way the theoretical uncertainties on the measurement of α_s to second order can be reduced to a negligible level.

In the next section, the data analysis, including the determination of the experimental value R_{EXP} , is briefly described. The calculation of the topological K-factors using the new theoretical input represents one of the main aspects of the present paper and is presented in section 3. The K-factors are used together with the Monte Carlo simulation of W production in section 4 to extract the Monte Carlo prediction, R_{MC} , for the α_s value used in the simulation. In section 5 the final result for α_s is determined and the systematic uncertainties are discussed.

2. DETERMINATION OF THE EXPERIMENTAL RATIO R_{EXP}

The upgraded UA2 experiment [2] at the CERN $p\bar{p}$ collider has collected large samples of $W \rightarrow e\nu$ and $Z \rightarrow e^+e^-$ events during the 1988, 1989 and 1990 running periods. In previous studies, some of these data have been used to measure the production cross sections of the W and Z bosons [6], their transverse momentum distributions [7] and precise values of their masses [8]. Details of the event samples and a brief description of the detector components relevant to electron identification can be found in Ref. [6] and references therein. In the present analysis the same identification criteria as described in Ref. [6] are used to select electron candidates in the central calorimeter ($|\eta| < 1.0$) and the same kinematic selection is applied to define a clean sample of $W \rightarrow e\nu$ events :

- $p_T^e > 20 \text{ GeV}$, $p_T^\nu > 20 \text{ GeV}$
- $M_T^{e\nu} > 40 \text{ GeV}$

where p_T^e is the transverse momentum of the electron candidate and p_T^ν is the missing transverse momentum attributed to the neutrino. $M_T^{e\nu}$ is the transverse mass of the electron-neutrino system, defined as $M_T^{e\nu} = \sqrt{2 p_T^e p_T^\nu (1 - \cos\Delta\phi)}$, where $\Delta\phi$ is the azimuthal separation between the measured electron and neutrino directions. These selection criteria are fulfilled by 2964 events which are then investigated for jet activity.

To identify jets in W events and to measure their energy, the same cone algorithm as described in Ref. [1] is used. In a first step, energy clusters are formed by adjacent calorimeter cells containing an energy of more than 400 MeV. The straight line joining the interaction vertex and the energy weighted cluster centroid is defined as the jet axis. The jet energy is then computed as the sum of the energies of all calorimeter cells whose centers are contained in a cone around this axis. All cells satisfying the condition $\sqrt{(\Delta\phi)^2 + (\Delta\eta)^2} < 0.7$, where $\Delta\phi$ (in rad) and $\Delta\eta$ are the azimuthal and pseudorapidity separation between the cell centre and the jet axis, are included in the energy sum. In order to define a jet the transverse energy is required to be above a given threshold E_T^0 and the jet axis must be contained in a given pseudorapidity range $|\eta| < \eta_{\text{cut}}$. To reduce the systematic uncertainties in the jet energy measurement and to decrease the number of jets arising from the interaction of spectator partons (underlying event), only those jets are retained whose transverse energy exceeds $E_T^0 = 20 \text{ GeV}$ and whose axis is contained in the pseudorapidity range $|\eta| < 1.6$. Using these cuts, 114 events with one jet and five events with two jets are found in the sample of 2964 W candidates.

These samples are slightly contaminated by two sources of background :

1. $W \rightarrow \tau\nu, \tau \rightarrow e\nu\bar{\nu}$ events, which pass the kinematical cuts. Their contribution to the W + zero-jet and the W + one-jet samples is evaluated using the same Monte Carlo program as for $W \rightarrow e\nu$ decays (see section 3). The background contamination is found to be 3.8% in the W + zero-jet sample and 3.3% in the W + one-jet sample. The slightly smaller contamination observed in the latter case is due to the larger inefficiency for finding the lower energy electrons from τ decays in the presence of jet activity.
2. Misidentified electrons from QCD jet production. The method used to estimate their contribution has already been described in Ref. [6]. By using a sample of π^0 candidates, the contributions were estimated to be $0.4 \pm 0.1\%$ in the W + zero-jet sample and $3.1 \pm 1.4\%$ in the W + one-jet sample. The larger fraction of background observed in the W + one-jet sample is expected, since these misidentified electrons arise from events containing two or more jets, where one of the jets is misidentified as an electron.

After background subtraction the experimental ratio is found to be :

$$R_{\text{EXP}} = \frac{\text{number of } W + \text{one-jet events}}{\text{number of } W + \text{zero-jet events}} = \frac{106.7 \pm 10.8}{2725.5 \pm 53.4} = 3.91 \pm 0.40\%.$$

3. K FACTOR CALCULATION

The QCD prediction for the W + jet rates is based on a Monte Carlo simulation of W production. The matrix elements of all tree diagrams up to order α_s^3 have been calculated [9] and are implemented in the framework of a Monte Carlo program (hereafter referred to as the EKS Monte Carlo). The infrared and collinear divergences, which show up in the higher order tree diagrams, are regularized by applying cutoffs on the transverse momenta, P_T , of each outgoing parton and on the angular separation ω of each pair of outgoing partons:

$$P_T > P_T^{\text{min}} \tag{1}$$

$$\omega > \omega^{\text{min}}$$

The EKS simulation represents only a partial calculation of the total W production cross section, because loop diagrams and tree diagrams with outgoing partons which do not fulfil the conditions (1) are not taken into account. The size of these missing contributions

is given by multiplicative corrections called K-factors. A complete definition of these is given in Ref. [1] and will not be repeated here.

The total cross section to second order in α_s can be written as

$$\sigma^{[2]} = \sigma_0 K_0 + \sigma_1 K_1 + \sigma_2 K_2 \quad (2)$$

where the σ_i are the tree level cross sections for the production of a W boson accompanied by i partons computed by the EKS Monte Carlo and K_i are the so called topological K-factors. The superscript in brackets indicates the order to which the perturbative calculation has been performed. This notation will be used throughout the following. The product $\sigma_i K_i$ is called a topological cross section and is characterized by the fact that exactly i partons ($i = 0,1,2$) fulfil the P_T^{\min} and ω^{\min} conditions (1). For example, contributions to K_1 arise from second order diagrams where only one parton fulfils the criteria while the second one is either soft or virtual. It can be shown [1] that the K-factors can be expressed as power series in α_s . If the perturbative calculation is performed up to second order they can be written as

$$K_0 = 1 + \alpha_s \xi_1 + \alpha_s^2 \xi_2 \quad (3)$$

$$K_1 = 1 + \alpha_s \eta_1$$

$$K_2 = 1.$$

For a complete QCD prediction of the W + jet rates these K-factors must be known. Since K_1 will be used to compute K_0 , the calculation of K_1 will be described first.

3.1 The calculation of K_1

This calculation is based on the calculation of the P_T^W distribution to order α_s^2 from Ref. [5]. For P_T^W values above P_T^{\min} a function $K_1(P_T^W)$ can be defined from the relation

$$\frac{d \sigma^{[2]}}{d P_T^W} = \frac{d \sigma_1}{d P_T^W} K_1(P_T^W) + \frac{d \sigma_2}{d P_T^W} \quad \text{for } P_T^W > P_T^{\min} \quad (4)$$

where the term on the left hand side corresponds to the total inclusive P_T^W spectrum and the differential cross sections on the right hand side are obtained from the tree level Monte Carlo calculations. The relation above implies that K_1 in eq. (2) is related to $K_1(P_T^W)$ via

$$K_1 = \frac{1}{\sigma_1} \int_{P_T^{\min}}^{\infty} \left[\frac{d \sigma_1}{d P_T^W} K_1(P_T^W) \right] d P_T^W \quad (5)$$

The K_0 term from Eq. (2) has been neglected. By neglecting this term it is assumed that the P_T^W spectrum above a P_T^0 value is completely given by configurations with at least one parton above the cutoff. This is exactly true for all P_T^W values above the value $P_T^0 \approx 2 P_T^{\min}$. For P_T^W values between P_T^{\min} and P_T^0 relation (4) is not exact and neglects contributions from second order diagrams where two outgoing partons are emitted and which fulfil the kinematical conditions

$$P_T^1 < P_T^{\min} \quad P_T^2 < P_T^{\min} \quad \omega > \omega^{\min} \quad P_T^W > P_T^{\min} .$$

However, due to the correlation between K_0 and K_1 imposed by eq. (2), the overall result for α_s is not significantly affected by this approximation. This is verified by a study of the dependence of α_s on the P_T^{\min} cut (see section 5).

For the calculation of $K_1(P_T^W)$, the EKS differential cross sections and $d\sigma^{[2]}/dP_T^W$ have to be determined in a consistent way. All cross sections have been computed in the \overline{MS} renormalization scheme, using $\mu = M_W$ as a scale. To derive a value for the strong coupling constant used in the matrix element calculation, the four flavour value of the QCD scale parameter Λ as given by the structure function parametrization has been converted to the corresponding five flavour value. In the present analysis the functional form of α_s given in Ref. [10] has been used to relate α_s and $\Lambda_{\overline{MS}}$.

The results of the K-factor calculation are shown in Fig. 1(a) for the structure function set HMRSB of Ref. [11] for three different P_T^{\min} values (6.0, 12.0 and 18.0 GeV). The angular cutoff ω^{\min} was fixed at 20° . Also shown is the curve obtained by ignoring the second order tree level contribution. In this case the function $K_1(P_T^W)$ corresponds to the ratio between the P_T^W spectrum calculated to second and first order. The results show a dependence of K_1 on P_T^W , which results from the fact that at large P_T^W values the second order tree level contribution is comparable in size to the first order tree level contribution. The sum of the two tree level cross sections is larger than the cross section from the complete second order calculation, leading to a K_1 value smaller than 1. This effect is particularly pronounced for small values of the cutoff parameter P_T^{\min} . Apart from the P_T^W dependence, K_1 depends on the cutoff values P_T^{\min} and ω^{\min} . The P_T^{\min} dependence is illustrated in the figure by the various curves. From the results of the previous analysis [1], the ω^{\min} dependence was shown to be small and has not been recalculated here. Furthermore, the function $K_1(P_T^W)$ shows a weak dependence on the choice of structure function, which is largely dominated by the α_s dependence, resulting from the different Λ values used in different sets of structure functions, as expected from eq. (3).

3.2 The Calculation of K_0

The calculation of K_0 is based on the calculation of the total K-factor to second order, $K_{\text{tot}}^{[2]}$, and uses in addition the results for K_1 obtained in the previous section. The total K factor at a given order is defined as the ratio between the total cross section and the Born term, so that $K_{\text{tot}}^{[2]}$ is given by

$$\sigma^{[2]} = K_{\text{tot}}^{[2]} \sigma_0. \quad (6)$$

This definition together with eq.(2) leads to

$$K_0 = K_{\text{tot}}^{[2]} - \frac{1}{\sigma_0} \int_{P_T^{\text{min}}}^{\infty} \left[\frac{d \sigma_1}{d P_T^W} K_1(P_T^W) \right] d P_T^W - \frac{\sigma_2}{\sigma_0} \quad (7)$$

The total K-factor has initially been calculated to first order in α_s in Ref. [12]. Recently, a complete calculation of $K_{\text{tot}}^{[2]}$ in the $\overline{\text{MS}}$ scheme has been performed in Ref. [4]. Using the HMRSB structure functions these calculations lead to the values 1.258 and 1.312 for the total K-factor in first and second order respectively [13]. The results of the calculation of K_0 , extracted by using the second order total K-factor, are shown as a function of P_T^{min} in Fig. 1(b). The corresponding value for the total K-factor is indicated by the dashed line. Owing to the dependence of σ_1 and σ_2 on P_T^{min} and ω^{min} , K_0 also depends on these cutoffs. The asymptotic behaviour for K_0 is obtained from eq. (7). For $P_T^{\text{min}} \rightarrow \infty$, the cross sections σ_1 and σ_2 vanish and K_0 approaches the value of the total K-factor calculated to second order.

4. DETERMINATION OF THE QCD PREDICTION R_{MC}

In order to obtain the QCD predictions for the W + jet rates, the K-factors are used in conjunction with the tree level Monte Carlo simulation of W production. Three sets of Monte Carlo events were generated with the EKS program according to the tree level cross sections σ_i ($i = 0,1,2$), representing the production of a W boson with 0, 1 and 2 partons. The parameters given in Table 1 were used for the EKS event generation. The outgoing partons (quarks and gluons) were fragmented according to the prescription of Ref. [14], where the parameters of the model were adjusted to describe the energy flow as measured experimentally for jets in W events. The additional hadronic activity in W events is found to be higher than in minimum bias events [7]. A very simple model to simulate this was used by superimposing two minimum bias events from UA2 data onto each generated hard scattering process. Due to the high energy threshold for the jet definition used in this analysis, the Monte Carlo predictions are relatively insensitive to the detailed simulation of the underlying event as discussed in the following section. Finally, the calorimeter response was simulated for all generated particles and the simulated events were subjected

to the same analysis chain as the real data. To each generated event class, the calorimetric electron identification and the kinematical cuts were applied leading to accepted cross sections, which are denoted as σ_i^{det} , where i is the number of partons.

Due to the experimental jet definition (E_T^0 and η cuts) and to acceptance and resolution effects, the number of jets passing the jet identification criteria in a simulated W event is not necessarily equal to the number of produced partons. Therefore, each accepted cross section σ_i^{det} splits into several components, characterized by the number of reconstructed jets in the event

$$\sigma_i^{\text{det}} = (\sigma_{i0} + \sigma_{i1} + \sigma_{i2} + \dots) \quad i = 0,1,2 \quad (8)$$

where σ_{ij} represents the cross section where i partons were generated and j jets were reconstructed after the detector simulation.

In order to extract R_{MC} , the P_T^W dependence of K_1 has to be taken into account by convoluting $d\sigma_1^{\text{det}} / dP_T^W$ with $K_1(P_T^W)$. For each partial cross section σ_{1j} factors K_{1j} can be defined :

$$\int_{P_T^{\text{min}}}^{\infty} \left[\frac{d\sigma_{1j}}{dP_T^W} K_1(P_T^W) \right] dP_T^W = K_{1j} \sigma_{1j} \quad j = 0,1,2. \quad (9)$$

The ratio R_{MC} is then given by

$$R_{\text{MC}}(\alpha_s^{\text{MC}}) = \frac{\sigma_{01} K_0 + \sigma_{11} K_{11} + \sigma_{21}}{\sigma_{00} K_0 + \sigma_{10} K_{10} + \sigma_{20}} \quad (10)$$

where α_s^{MC} is the α_s value used in the Monte Carlo simulation.

The following results for the various K -factors were found, using the input parameters given in Table 1 and the values for E_T^0 and η_{cut} quoted in section 2:

$$K_0 = 1.15$$

$$K_{10} = 1.54 \quad \text{and} \quad K_{11} = 1.35$$

Owing to the P_T^W dependence of K_1 the K_{10} and K_{11} values depend on E_T^0 and η_{cut} . The value of K_{11} is found to be smaller than the value of K_{10} since the cross section σ_{11} is dominated by events having a large P_T^W , where $K_1(P_T^W)$ is small.

The QCD predictions of R_{MC} are compared in Fig. 2 to the experimentally measured values for different η_{cut} and E_T^0 values. They are found to be consistent with the experimentally measured ratios and the η and E_T^0 dependence of R is well described. The Monte Carlo simulation also provides a good description of the transverse energy spectrum of the jets. The distribution of the measured jet transverse energies is shown in Fig. 3 for the 114 one-jet events with a transverse energy greater than 20 GeV. The spectrum predicted by the Monte Carlo simulation is superimposed on the data. It should be noted that the QCD predictions in Figs. 2 and 3, obtained with $\alpha_s^{MC} = 0.110$, are systematically lower than the experimentally measured values, indicating that a larger α_s -value than α_s^{MC} is needed to describe the data.

The observed rate for $W +$ two-jet events is found to be 4.7 ± 2.2 events after background subtraction, to be compared to the theoretical prediction of 2.3 events. Since the Monte Carlo calculation is performed to second order in α_s , the theoretical prediction for the $W + 2$ -jet rate corresponds to a leading order prediction ($K_2 = 1$) and no higher order corrections are taken into account.

5. DETERMINATION OF α_s AND SYSTEMATIC UNCERTAINTIES

In order to extract a measurement of α_s the equation

$$R_{MC}(\alpha_s) = R_{EXP} \quad (11)$$

has to be solved, which implies that the α_s dependence of the Monte Carlo ratio has to be known. This dependence results from two different contributions. Firstly, there is a direct dependence of the matrix elements on α_s resulting in a direct proportionality of the tree level cross sections σ_i to α_s^i as well as in the α_s dependence of the K -factors given in eq. (3). Secondly, since the cross sections σ_i depend on structure functions evolved to the relevant Q^2 values, an indirect dependence on α_s is introduced via the evolution equations. Whereas the matrix element dependence can be taken into account in a straightforward way, this is not possible for the structure function dependence. Due to the correlations between the parton distributions and the value of the QCD scale parameter Λ within a given structure function parametrization, it is not possible to change the Λ value independently from the form of the parton distributions. For a given structure function parametrization, the Λ value determined in the fit to the deep inelastic lepton nucleon data has to be respected and only one prediction for R_{MC} , corresponding to the α_s value given by the value of Λ , can be extracted.

In order to overcome this difficulty, structure function parametrizations were obtained for different Λ values. The fits were performed to the deep inelastic data sets used for the HMRSB parametrization in the $\overline{\text{MS}}$ scheme with Λ values of 0.100, 0.190 (standard HMRSB) and 0.300 GeV [15]. The K-factor calculation, as well as the full Monte Carlo simulation, were then performed for all three structure function sets leading to Monte Carlo predictions for R_{MC} at three different α_s values. The results of the calculations for R_{MC} are shown as a function of α_s in Fig. 4. The experimentally measured value R_{EXP} is indicated as a dashed line together with a band representing the statistical uncertainties. The dependence of R_{MC} on α_s is well approximated by a linear fit, leading by extrapolation to the result

$$\alpha_s(M_W^2) = 0.123 \pm 0.018 \text{ (stat.)}$$

At this point it should be noted that the procedure in which the α_s dependence of the structure functions is ignored [1] and only the dependence of the matrix elements is taken into account results in a stronger α_s dependence of R_{MC} and leads to an underestimate of the statistical error. The weaker α_s dependence of R_{MC} found by applying the correct procedure is due to a partial compensation of the increase in the cross section for higher α_s values by the modified parton distributions. This compensation is due to the correlation between the value of Λ and the shape of the gluon distribution used in the parametrization of the structure functions.

The extracted α_s result is still affected by various sources of systematic uncertainties which will be discussed in the following:

(a) As mentioned in section 4, differences in reconstruction efficiencies for electrons in $W + \text{jet}$ events with respect to $W + \text{zero-jet}$ events, are taken into account in the simulation for the calorimetric electron identification. However, tracking and preshower cut efficiencies might also be affected by the increased complexity in $W + \text{jet}$ events. It has been checked that such effects yield a negligible contribution to the systematic uncertainty on α_s , using a similar method to that described in Ref. [6] to measure these efficiencies from the W data sample.

(b) To search for a possible systematic effect coming from the jet algorithm, the jet identification criteria were changed and the α_s evaluation repeated. First, standard UA2 clusters [16] instead of cones were used to measure the jet energy, then the cluster algorithm was modified to perform the clustering in transverse energy rather than in energy. In each case, the observed change in α_s was found to be compatible with statistical fluctuations, providing no evidence for a systematic effect.

(c) The absolute energy scale of the UA2 calorimeter has an uncertainty of $\pm 1\%$ for the electromagnetic and $\pm 2\%$ for the hadronic compartment. The effects of these uncertainties on the α_s result were determined by varying the energy scale in the Monte Carlo calculation, resulting in a systematic error of

$$\Delta \alpha_s = \pm 0.005.$$

(d) Uncertainties in the calorimeter response to low energy particles were estimated by modifying the parametrizations of the response to hadrons as measured in test beams in the momentum range below 4.0 GeV. Extreme variations were chosen in such a way that the systematic uncertainties related to the low energy points (with a pion momentum down to 300 MeV) were taken into account. From this variation the systematic error is estimated to be

$$\Delta \alpha_s = \pm 0.003.$$

(e) The jet energy scale and the number of jets reconstructed in the detector are affected by the underlying event. Two different effects, which depend strongly on the minimal energy E_T^0 required in the jet definition, play an important role:

- jets can be reconstructed from the underlying event and contribute significantly to the one-jet rate via the cross section σ_{01} . The rate of jets in a superposition of two minimum bias events is found to be exponentially decreasing with E_T^0 and is below 0.1 % for E_T^0 values above 17 GeV.
- the jet energy measured in clusters or cones is increased by the underlying event contribution in the calorimeter cells included in the energy calculation.

To study the corresponding systematic effect on the α_s result, the underlying event simulation was modified such that only one UA2 minimum bias event was superimposed, even though this is known to be inconsistent with the observed energy flow. If, nevertheless, the observed differences in the extracted α_s result are taken conservatively as a systematic error resulting from uncertainties in the underlying event simulation, one obtains

$$\Delta \alpha_s = \pm 0.011.$$

(f) In order to estimate the uncertainties in α_s resulting from uncertainties in the structure functions, the analysis was repeated by using different parametrizations. The results found by using the HMRSE [11], MRSB' and MRSE' [17] and the DFLM [18]

parametrizations did not deviate by more than ± 0.005 , so that the systematic error is taken to be

$$\Delta \alpha_s = \pm 0.005.$$

(g) To estimate the systematic error arising from uncertainties in the fragmentation model, the results for α_s obtained by using various parameter settings in the fragmentation model have been compared. The parameters were varied to allow for changes in the energy flow around the jet axis and in the cluster radius distribution, which were barely compatible with the experimentally observed distributions. The variations found in the α_s result lead to

$$\Delta \alpha_s = \pm 0.010.$$

(h) In the previous analysis the α_s result showed a systematic dependence on the cutoff parameter P_T^{\min} used in the Monte Carlo generation [1]. Due to the improved K-factor calculations performed in the present analysis, this dependence has been reduced to a negligible level. A variation of $\Delta \alpha_s = \pm 0.002$ is found if P_T^{\min} is varied from 12 to 18 GeV.

Combining in quadrature the various contributions to the systematic error, as listed in Table 2, leads to the result :

$$\alpha_s (M_W^2) = 0.123 \pm 0.018 \text{ (stat.)} \pm 0.017 \text{ (syst.)}.$$

Due to the complete theoretical calculation of W production in second order QCD, leading to the improved K-factor calculation, the additional theoretical error of ± 0.020 , quoted in the previous analysis [1], has disappeared.

In order to illustrate the sensitivity of the α_s measurement to a change of the renormalization scale μ , the α_s determination has been repeated for the choice $\mu = M_W/2$ instead of $\mu = M_W$. This variation resulted in a change of $\alpha_s (M_W^2)$ by $\Delta \alpha_s = - 0.010$.

The present result can be compared to recent experimental determinations of α_s in e^+e^- experiments at $\sqrt{s} = M_Z$. The relative production rates of multijet hadronic final states of Z decays have been used [19] to extract a measurement of $\alpha_s (M_Z^2)$ in the $\overline{\text{MS}}$ scheme. These analyses lead to α_s results in the range between 0.114 and 0.124 with typical errors, combining statistical and systematic uncertainties, of $\Delta \alpha_s = \pm 0.008$. In recent analyses $\alpha_s (M_Z^2)$ has also been extracted from measurements of the asymmetry of energy-energy correlations [20,21,22]. The values obtained are : $\alpha_s (M_Z^2) = 0.117 \pm 0.009$ [20],

$\alpha_s (M_Z^2) = 0.106 \pm 0.005$ [21] and $\alpha_s (M_Z^2) = 0.117 \pm 0.005$ [22], where the respective experimental and theoretical errors are added in quadrature. In addition, α_s has been measured from global event shape variables in hadronic Z decays [23], leading to the result: $\alpha_s (M_Z^2) = 0.121 \pm 0.008$.

6. CONCLUSIONS

From a study of W + jet production in the UA2 experiment at the CERN $p\bar{p}$ collider a second order determination of the strong coupling constant α_s in the \overline{MS} scheme has been performed. The measurement of the ratio between the W + one-jet and W + zero-jet event rates leads to

$$\alpha_s (M_W^2) = 0.123 \pm 0.018 \text{ (stat.)} \pm 0.017 \text{ (syst.)}.$$

The present result is in agreement with recent determinations of α_s in e^+e^- experiments at $\sqrt{s} = M_Z$. Although the precision obtained at e^+e^- colliders cannot be reached, the present analysis provides an independent measurement of the strong coupling constant in a hadronic collision experiment from a process in which α_s is determined from gluon radiation in the initial state.

ACKNOWLEDGEMENTS

We thank our theory colleagues T. Matsuura, R.G. Roberts and W.J. Stirling for fruitful discussions and for providing us detailed results of their calculations.

We gratefully acknowledge P. Darriulat for his contribution and guidance during the design and construction of the UA2 upgrade project.

The technical staff of the institutes collaborating in UA2 have contributed substantially to the construction and operation of the experiment. We deeply thank them for their continuous support. The experiment would not have been possible without the very successful operation of the improved CERN $p\bar{p}$ Collider whose staff and coordinators we sincerely thank for their collective effort. Financial support from the Schweizerischen Nationalfonds zur Förderung der Wissenschaftlichen Forschung to the Bern group, from the UK Science and Engineering Research Council to the Cambridge group, from the Bundesministerium für Forschung und Technologie to the Dortmund and Heidelberg groups, from the Australian Research Council, the CRA Pty Ltd, and the Victorian Education Foundation to the Melbourne group, from the Institut National de Physique Nucléaire et de Physique des Particules to the Orsay group, from the Istituto Nazionale di Fisica Nucleare to the Milano, Pavia, Perugia and Pisa groups and from the Institut de Recherche Fondamentale (CEA) to the Saclay group are acknowledged.

REFERENCES

- [1] UA2 Collaboration, R. Ansari et al., Phys. Lett. B215 (1988) 175.
- [2] UA2 Collaboration, Proposal to improve the performance of the UA2 detector, CERN/SPSC 84-30,84-95 and 85-3 (1984 and 1985, unpublished);
UA2 Collaboration, C.N. Booth, Proc. 6th Topical Workshop on Proton Antiproton Collider Physics, Aachen 1986.
- [3] T. Matsuura, W.L. van Neerven, Z. Phys. C38 (1988) 623;
T. Matsuura, S.C. van der Marck, W.L. van Neerven, Phys. Lett. B211 (1988) 171 and Nucl. Phys. B319 (1989) 570.
- [4] R. Hamberg, W.L. van Neerven, and T. Matsuura, DESY 90-129 (1990).
- [5] P.B. Arnold, M.H. Reno, Nucl. Phys. B319 (1989) 37.
- [6] UA2 Collaboration, J. Alitti et al., Z. Phys. C47 (1990) 11.
- [7] UA2 Collaboration, J. Alitti et al., Z. Phys. C47 (1990) 523.
- [8] UA2 Collaboration, J. Alitti et al., Phys. Lett. B241 (1990) 150.
- [9] S.D. Ellis, R. Kleiss, W.J. Stirling, Phys. Lett. B154 (1985) 435;
F.A. Berends, W.T. Giele and H. Kuijf, Nucl. Phys. B321 (1989) 39;
F.A. Berends, W.T. Giele, H. Kuijf, R. Kleiss, and W.J. Stirling, Phys. Lett. B224 (1989) 237.
- [10] Review of Particle Properties, Phys. Lett. B239 (1990) III.51.
- [11] P.N. Harriman, A.D. Martin, R.G. Roberts, W.J. Stirling, Durham University DTP/90/04 (revised version April 1990).
- [12] G. Altarelli et al., Nucl. Phys. B246 (1984) 12;
G. Altarelli et al., Z. Phys. C27 (1985) 617.
- [13] T. Matsuura, private communication, Nov. 1990.
- [14] R.D. Field, R.P. Feynman, Nucl. Phys. B138 (1978) 1.

- [15] R.G. Roberts and W.J. Stirling, private communication, June 1990.
- [16] UA2 Collaboration, M. Banner et al., Phys. Lett. B118 (1982) 203.
- [17] A.D. Martin, R.G. Roberts, W.J. Stirling Phys. Lett. B206 (1988) 327 and Mod. Phys. Lett. A4 (1989) 1135.
- [18] M. Diemoz, F. Ferroni, E. Longo, and G. Martinelli, Z. Phys. C39 (1988) 21.
- [19] MARK II Collaboration, S. Komamiya et al., Phys. Rev. Lett. 64 (1990) 987;
 OPAL Collaboration, M.Z. Akrawy et al., Phys. Lett. B235 (1990) 389;
 DELPHI Collaboration, P. Abreu et al., Phys. Lett. B247 (1990) 169;
 L3 Collaboration, B. Adeva et al., Phys. Lett. B248 (1990) 464;
 OPAL Collaboration, M.Z.Akrawy et al., CERN-PPE/90-143.
- [20] OPAL Collaboration, M.Z. Akrawy et al., Phys. Lett. B252 (1990) 159.
- [21] DELPHI Collaboration, P. Abreu et al., Phys. Lett. B252 (1990) 149.
- [22] ALEPH Collaboration, D. Decamp et al., CERN-PPE/90-196.
- [23] ALEPH Collaboration, D. Decamp et al., Phys. Lett. B255 (1991) 623.

Table 1 : List of parameters used in the EKS Monte Carlo simulation

Parton level cuts:	$P_T^{\min} = 12 \text{ GeV}$
	$\omega^{\min} = 20^\circ$
Matrix elements:	$\mu = M_W = 80.5 \text{ GeV}$
	$\Gamma_W = 2.1 \text{ GeV}$
	$\Lambda_{\overline{\text{MS}}}^{(4)} = 0.190 \text{ GeV}$ (for HMRSB)
	$\Rightarrow \Lambda_{\overline{\text{MS}}}^{(5)} = 0.122 \text{ GeV}$
	$\alpha_s = \alpha_s^{[2]} = 0.110$ (for HMRSB)

Table 2 : Summary of systematic errors

energy scale	± 0.005
low energy response	± 0.003
underlying event	± 0.011
structure functions	± 0.005
fragmentation	± 0.010
theoretical uncertainties	± 0.002
total systematic error	± 0.017

FIGURE CAPTIONS

- Fig. 1. (a) K_1 as a function of P_T^W for different P_T^{\min} values (dashed curves). The ratio between the second and first order P_T^W spectrum is represented by the solid line. (b) K_0 as a function of P_T^{\min} ; The value of the second order total K-factor is indicated by the dashed line. In the calculation of both, K_1 and K_0 the structure function set HMRSB of Ref. [11] has been used.
- Fig. 2. R_{MC} and R_{EXP} as a function of the rapidity cut η for E_T^0 cuts of 20 and 25 GeV. The structure function set used is HMRSB of Ref. [11] with $\alpha_s^{MC} = 0.110$.
- Fig. 3. Spectrum of transverse energies of jets from data as compared with the Monte Carlo prediction for the jet cuts $E_T^0 = 20$ GeV and $\eta_{cut} = 1.6$. The structure function set used is HMRSB of Ref. [11] with $\alpha_s^{MC} = 0.110$.
- Fig. 4. $R_{MC}(\alpha_s)$ compared to the experimental measurement R_{EXP} . The QCD predictions R_{MC} have been calculated by using three different HMRSB structure function parametrizations with three different values for Λ .

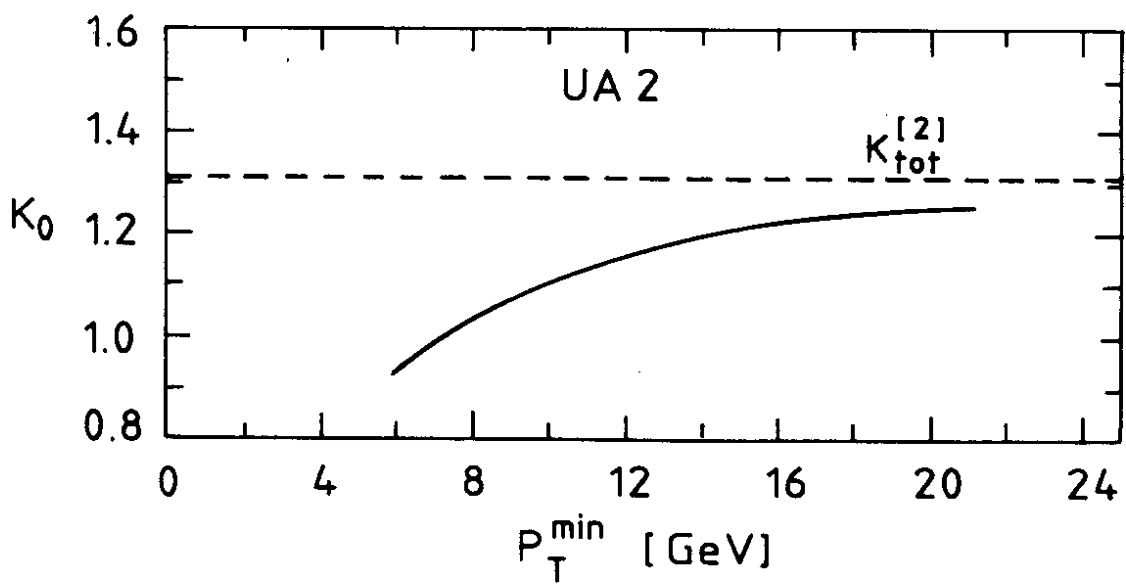
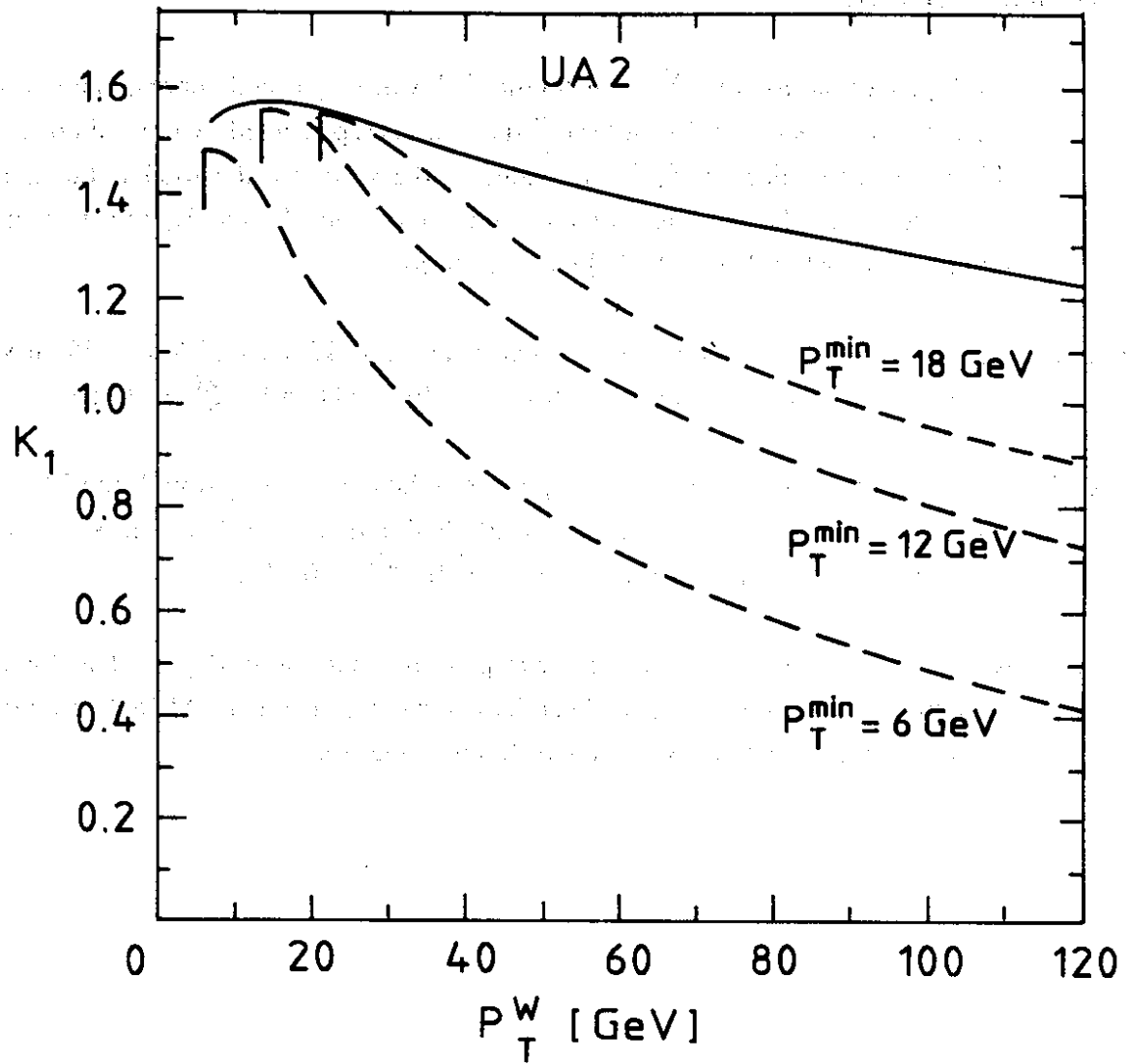


Fig. 1

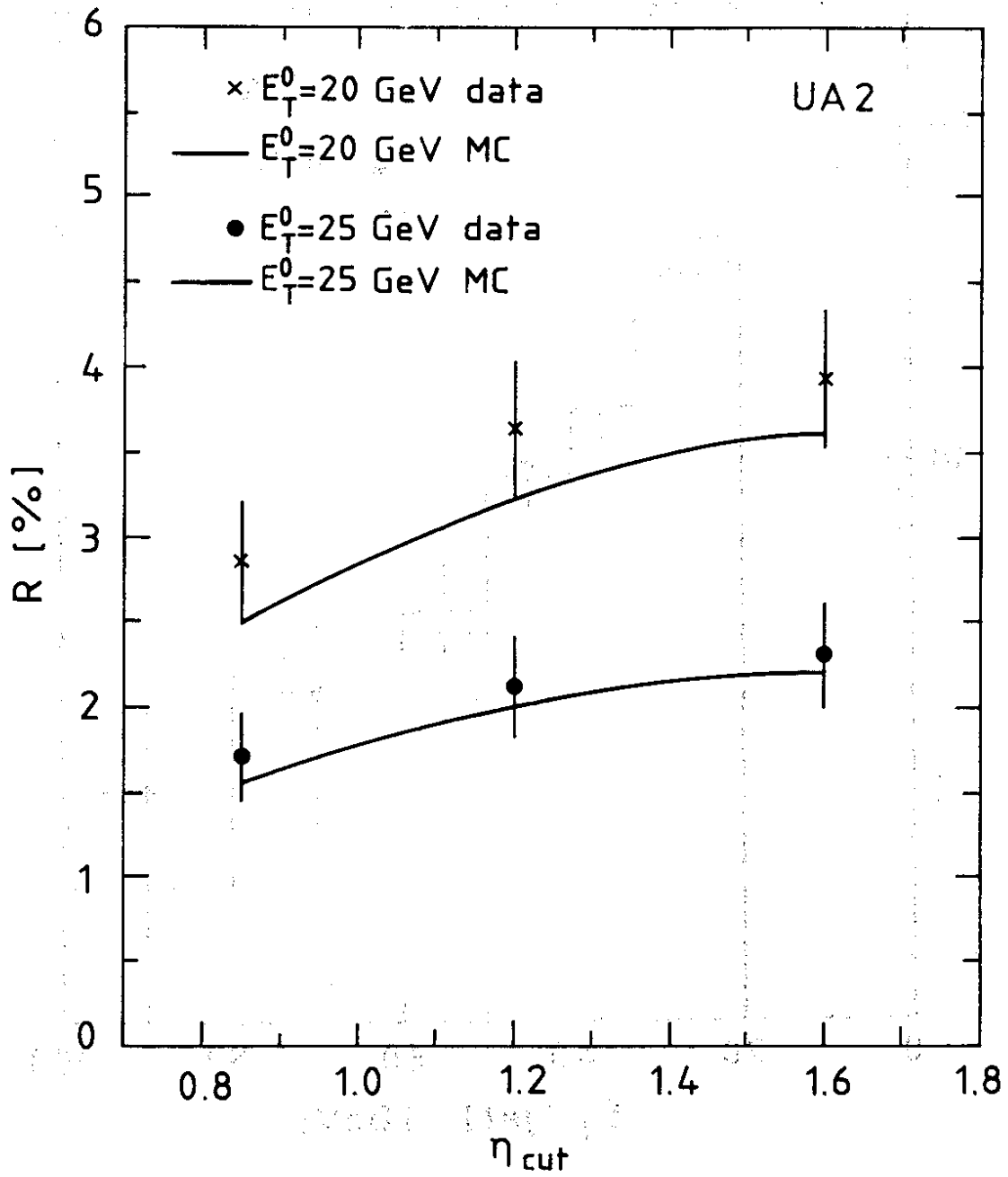


Fig. 2

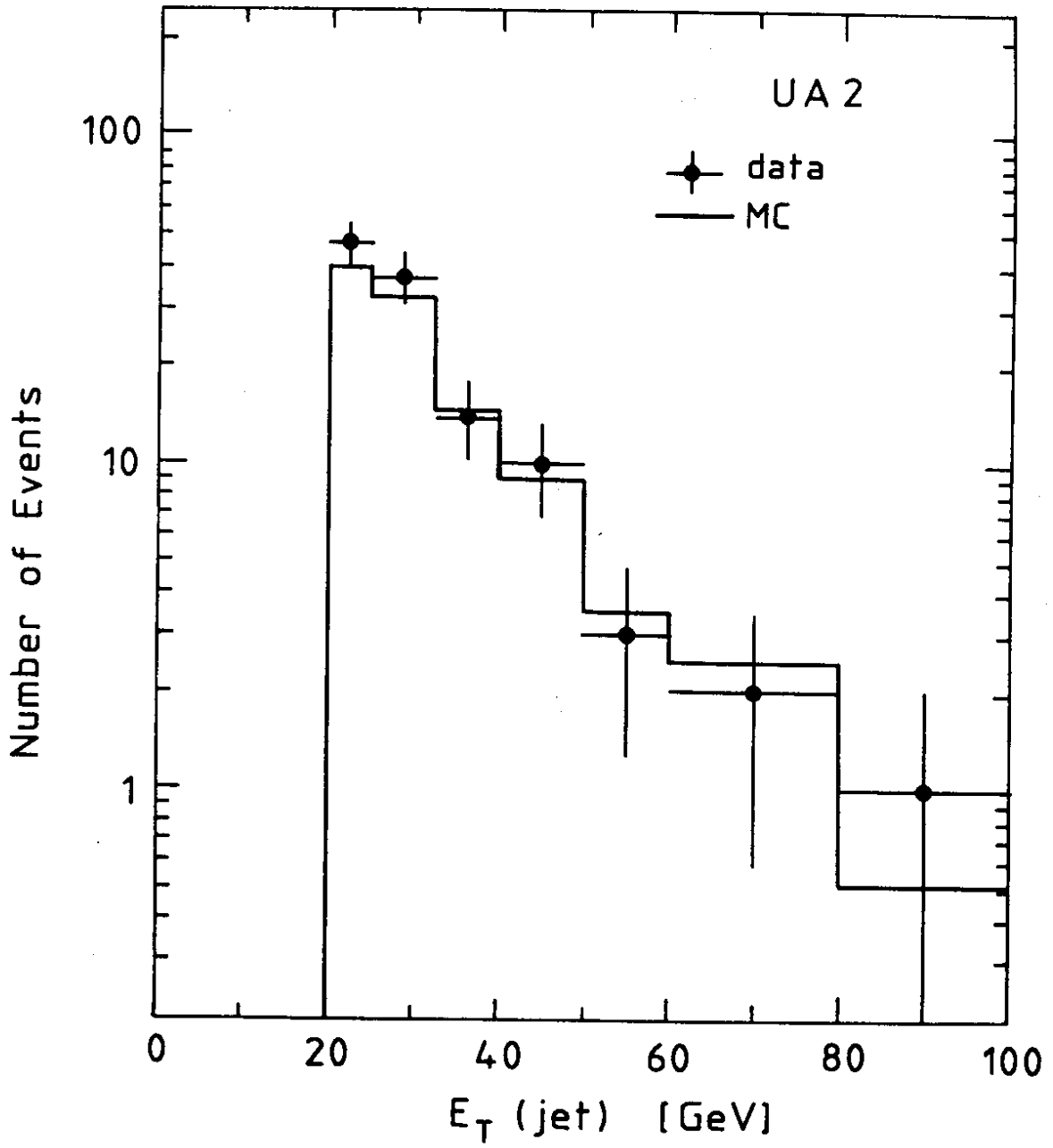


Fig. 3

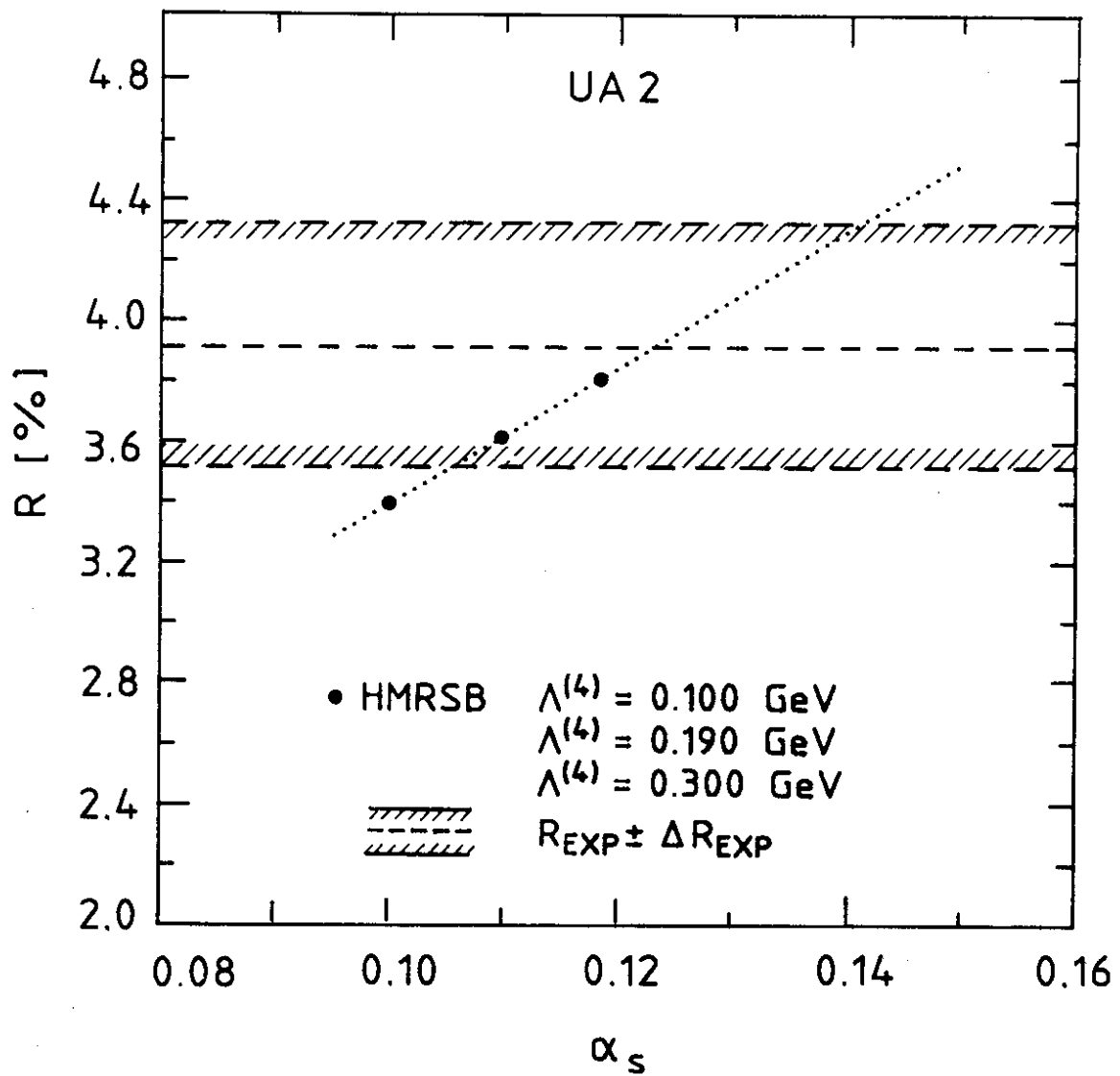


Fig. 4